

# A Numerical Method for Schwarz-Christoffel Conformal Transformation with Application to Potential Flow in Channels with Oblique Sub-channels

P.M.J. Trevelyan<sup>1</sup>, L. Elliott<sup>1</sup>, D.B. Ingham<sup>1</sup>

**Abstract:** The potential flow in a semi-infinite channel with multiple semi-infinite oblique sub-channels is determined using the Schwarz-Christoffel transformation and complex potential theory. The standard iterative technique, i.e. the Newton-Raphson method with the Jacobian matrix approximated by a finite-difference quotient matrix, was employed with an alternative integration region to that found elsewhere in the literature is employed after integrating across the boundaries to determine the Schwarz-Christoffel transformation parameters which solely depend on the dimensions of the region being considered. Each semi-infinite channel permits integration at infinity perpendicularly across the channel and sub-channels, yielding some analytical relationships between these parameters. The remainder of the parameters requires the use of numerical integration, which in the present situation was the Runge-Kutta-Merson method. Once these parameters were determined the Schwarz-Christoffel transformation was integrated numerically using a variable-step Adams method and this completes the mapping from the region being considered to the upper half of the complex plane. This technique employed is illustrated by considering a semi-infinite channel with an inlet and an outlet attached to the top and the side of the channel, respectively, with both these sub-channels at prescribed oblique angles to the main channel. The whole region is modelled by a semi-infinite channel with two sub-channels attached, all of which have uniform flows at infinity.

**keyword:** Schwarz-Christoffel, boundary integral method, oblique channels, potential flow.

## 1 Introduction

In this paper we investigate the 2D potential fluid flow inside a semi-infinite channel with various inlets and outlets each supplying a uniform flow of fluid. However, without any loss of generality, the situation investigated in this paper is restricted to a channel attached to the top of the main channel at an angle  $\beta\pi$  to the normal to the channel and a channel attached to the end of the main channel at an angle  $\alpha\pi$  to the normal to the channel, see Fig. 1, on which the various dimensions of the different channels are clearly indicated.

Physically we are investigating the potential flow in a long room with two ducts, namely one oblique ventilation duct attached to the ceiling and one oblique extraction duct attached

to a wall of the room. The opposite wall of the room is assumed to be porous and through which a uniform flow can be introduced. This combined system corresponds to a room ventilation situation, see Fletcher and Johnson (1992).

Whilst locally sources and sinks produce radial flows, when they are placed in channels the fluid flow approaches uniform flow at large distances from the source and sink. This leads to the introduction of semi-infinite channels being used to model finite ducts, with each channel introducing three new parameters and a global analytical parameter relationship into the Schwartz-Christoffel transformation. Further, an approximate relationship is found for the local parameters of each sub-channel.

To model this problem we use 2D potential flow in which the long room with the porous wall is replaced by a semi-infinite channel and the two finite ducts are replaced by semi-infinite sub-channels. To calculate the potential flow inside the channel with inlet and outlet sub-channels, a region which we denote by  $G_z$ , we have chosen to map  $G_z$  using the Schwarz-Christoffel transformation onto the region  $G_\zeta$  which corresponds to the upper half of the complex  $\zeta$  plane. The fluid flow in the region  $G_\zeta$  is then easily established and from this the stream function and fluid velocities in  $G_z$  can readily be determined. The  $x$ ,  $y$ ,  $\xi$  and  $\eta$  axes are taken as the horizontal and vertical directions in the  $z$  plane and  $\zeta$  planes, respectively.

The Schwarz-Christoffel transformation involves several unknown parameters which must be determined before the mapping can be applied. All the previous works determine these parameters using various integration methods along the real axis of the  $\zeta$  plane, together with some form of iterative procedure. Two examples of such methods are presented in Gribnyak, Logvinenko, Romanenko, Fedorovich and Ennan (1991) and Chaung, Gui and Hsiung (1993). The most used iterative procedure is the Newton-Raphson method, with the Jacobian matrix approximated by a finite-difference quotient matrix, as applied to branched channels by Hassenpflug (1998). There are also applications to problems involving 2D free surface flows over obstacles, with the aim of determining the downstream free surface, see Abdelmalek (1994) who considered a free waterfall at high Froude number based on conditions far upstream, and a large number of recent applications to 2D electromagnets, see Minuhin (1993).

This paper mainly relates to an alternative integration approach from that employed by Hassenpflug (1998) in the it-

<sup>1</sup> Department of Applied Mathematics, University of Leeds, LS2 9JT, UK.

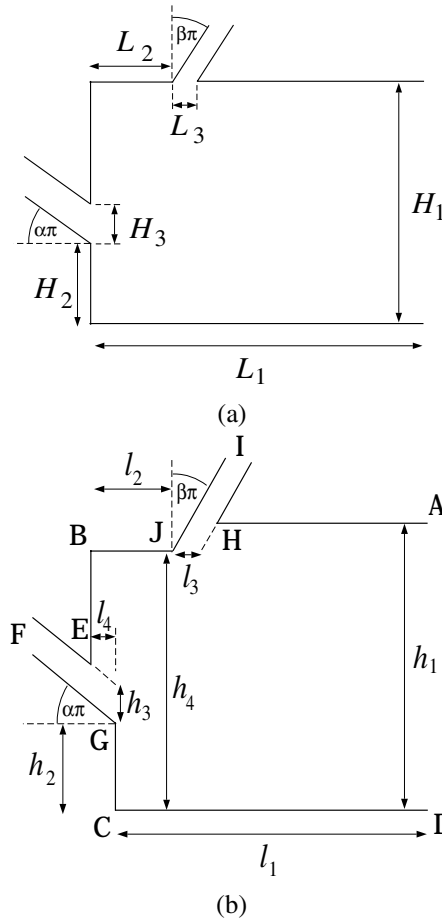


**Figure 1 :** (a) A schematic diagram of the model of the room with an inlet and outlet, (b) the boundary of  $G_z$  with the lengths  $h_1, h_2, h_3, h_4, l_1, l_2, l_3$  and  $l_4$  indicated. The points A, D, I and F are at infinity in the complex  $z$  plane.

erative mathematical technique for determining the parameters involved in the Schwarz-Christoffel transformation. This method calculates the lengths using integrals in the  $z$  plane as opposed to in the  $\zeta$  plane, which gives rise to some analytical relationships between the parameters wherever there are semi-infinite sub-channels. Hence, we only consider simply connected unbounded polygonal domains. In order to calculate the potential flow inside such regions we map the entire flow domain onto the upper half of the complex plane using the Schwarz-Christoffel transformation and then determine the fluid flow in the upper half of that complex plane. In comparison to the use of finite-difference and finite element methods, this procedure saves on cpu time as at this stage no iteration procedure is required to determine the fluid flow once the transformation involving all the parameters has been established.

## 2 Semi-infinite Multi-Channel Domain

The Schwarz-Christoffel theorem states that if  $\zeta_1, \zeta_2, \dots, \zeta_n$  are  $n$  finite points on the real axis in the  $\zeta$  plane such that  $\zeta_1 < \zeta_2 < \dots < \zeta_n$  and  $\theta_1, \theta_2, \dots, \theta_n$  are the interior angles of a simple closed polygon of  $n+1$  vertices in the  $z$  plane, then the transformation from the  $\zeta$  plane to the  $z$  plane is defined by

$$\frac{dz}{d\zeta} = K(\zeta - \zeta_1)^{\frac{\theta_1}{\pi}-1}(\zeta - \zeta_2)^{\frac{\theta_2}{\pi}-1} \dots (\zeta - \zeta_n)^{\frac{\theta_n}{\pi}-1} \quad (1)$$

It should also be noted that the constant  $K$  may be complex, but throughout this paper it is taken to be real since no rotations of the planes are required. Each quantity  $\zeta_i$  is real and is mapped onto the vertex in  $G_z$ , where the interior angle is  $\theta_i$ . Without any loss of generality we can choose the values of two of these  $\zeta_i$ 's.

In order to use the Schwarz-Christoffel theorem, the values of  $\zeta$  which are mapped to the corners of  $G_z$  are required. Unfortunately, these values of  $\zeta$  are unknown, so initially they have to be estimated and then the Schwarz-Christoffel theorem can be used to map  $G_z$  to  $G_\zeta$ . In performing this mapping we create a region  $G_z$  with all the correct angles at the corners but with dimensions not having the same magnitudes as those shown in Fig. 1(a), which have the lengths  $H_1, H_2, H_3, L_1, L_2$  and  $L_3$ . So the lengths  $h_1, h_2, h_3, h_4, l_1, l_2, l_3$  and  $l_4$  are introduced and are shown in Fig. 1(b). In the numerical procedure described in this paper an iterative scheme is employed which ensures that all these lengths converge to the required values, namely,  $h_i$  and  $l_i$  tend to  $H_i$  and  $L_i$ , respectively, for  $i = 1, 2$  and  $3$ , and  $h_4$  and  $l_4$  tend to  $H_1$  and to zero, respectively. The lengths  $h_4$  and  $l_4$  are introduced to define the region shown in Fig. 1(b).

The points A and D at infinity in the  $z$  plane are mapped to  $-\infty$  and  $\infty$  in the  $\zeta$  plane, respectively. We consider the whole region as shown in Fig. 1, where  $G_z$  is an infinite channel with three discontinuities in the height of the channel, one along the bottom and two along the top of the channel. The 8 corners in  $G_z$  are H, I, J, B, E, F, G and C, which are mapped to the points  $-\xi_H, -\xi_I, -\xi_J, -\xi_B, 0, 1$  and  $\xi_C$  in  $G_\zeta$ , respectively. The interior angles at B and C are both  $\frac{\pi}{2}$ , at H, J, E and G they are  $(\frac{3}{2} + \beta)\pi, (\frac{3}{2} - \beta)\pi, (\frac{3}{2} + \alpha)\pi$  and  $(\frac{3}{2} - \alpha)\pi$ , respectively, and at I and F are both zero. Hence, we have

$$\frac{dz}{d\zeta} = \frac{K(\zeta - 1)^{\frac{1}{2}-\alpha}(\zeta + \xi_E)^{\frac{1}{2}+\alpha}(\zeta + \xi_J)^{\frac{1}{2}-\beta}(\zeta + \xi_H)^{\frac{1}{2}+\beta}}{\zeta(\zeta + \xi_I)(\zeta + \xi_B)^{\frac{1}{2}}(\zeta - \xi_C)^{\frac{1}{2}}} \quad (2)$$

which maps  $G_z$  to  $G_\zeta$ .

Before solving the differential equation (2), the parameters  $\xi_B, \xi_C, \xi_E, \xi_H, \xi_I, \xi_J$  and  $K$ , need to be determined so that the lengths  $h_1, h_2, h_3, h_4, l_1, l_2, l_3$  and  $l_4$  achieve their required values.

## 3 Integration Techniques

The first-order complex ordinary differential equation (2) has to be solved so that the mapping from  $G_z$  to the  $G_\zeta$  may be

found. This equation cannot be integrated analytically and therefore a numerical approach is required. This equation is of the form

$$\frac{dz}{d\zeta} = f_g(\zeta) \quad (3)$$

which if solved numerically maps  $G_\zeta$  to  $G_z$  but we require  $G_z$  to be mapped onto  $G_\zeta$ . Simply by inverting Eq. (3) we obtain

$$\frac{d\zeta}{dz} = f(\zeta) \quad (4)$$

where, for convenience,  $1/f_g(\zeta)$  is replaced by the function  $f(\zeta)$ , and this new equation ensures that when solving numerically with  $z$  chosen then the value of  $\zeta$  is found. Using this new formulation, the governing equation (2) can be inverted into the form of Eq. (4), which implies that we now have the governing differential equation

$$\frac{d\zeta}{dz} = \frac{\zeta(\zeta + \xi_I)(\zeta + \xi_B)^{\frac{1}{2}}(\zeta - \xi_C)^{\frac{1}{2}}}{K(\zeta - 1)^{\frac{1}{2}-\alpha}(\zeta + \xi_E)^{\frac{1}{2}+\alpha}(\zeta + \xi_J)^{\frac{1}{2}-\beta}(\zeta + \xi_H)^{\frac{1}{2}+\beta}} \quad (5)$$

By applying the Cauchy-Riemann equations to Eq. (4), with  $f = f_{\Re} + i f_{\Im}$ , the complex differential equation reduces to these two real ordinary differential equations

$$f_{Re} = \frac{\partial \xi}{\partial x} = \frac{\partial \eta}{\partial y} \quad \text{and} \quad f_{Im} = \frac{\partial \eta}{\partial x} = -\frac{\partial \xi}{\partial y} \quad (6)$$

But these only allow integration in the horizontal and vertical directions, however, by a rotation of the  $z$  plane by defining

$$\tilde{z} = z e^{i\gamma} \quad \text{and} \quad \tilde{f} = e^{-i\gamma} f \quad (7)$$

alters Eq. (4) to

$$\frac{d\zeta}{d\tilde{z}} = \tilde{f} \quad (8)$$

This allows integrations at an arbitrary angle. So that for changes in the new variable  $\tilde{x}$  in  $G_{\tilde{z}}$ ,  $\Delta\tilde{z} = \Delta\tilde{x}$ , Eq. (6) implies that

$$\tilde{f}_{\Re} = \frac{d\xi}{d\tilde{x}} \quad \text{and} \quad \tilde{f}_{\Im} = \frac{d\eta}{d\tilde{x}} \quad (9)$$

with similar expressions for changes in  $\tilde{y}$ .

Hence, by applying the Cauchy-Riemann equations, we separated the first-order complex differential equation into two real and imaginary first-order ordinary differential equations, allowing integration along lines at an arbitrary angle by a rotation of the plane. In order to obtain accurate solutions of the governing equation, the numerical integration of this pair of first-order real differential equations was performed with the aid of the NAG Fortran library.

In the parameter determination process the initial value NAG routine D02BGF was employed which integrates a system of first-order differential equations, subject to suitable initial conditions, over an interval using a Runge-Kutta-Merson method until a specified variable attains a given value. However, to map region  $G_z$  to  $G_\zeta$  then the routine D02CJF was preferred since this routine integrates a system of first-order differential equations, with suitable initial conditions, over a given range using a variable-order, variable-step, Adams method until a supplied user-specified function of the solution is zero. It then returns the solution at the points in the range specified by the user.

### 3.1 Integral boundary condition

When the boundary conditions are given at singular points, namely E, G, H and J, the NAG routines require values near the singular points which are obtained using expansions for  $\zeta$  in terms of  $z$  near the corners. For example, the function  $f$  is not defined at  $\zeta = 1$ , but the point G, namely  $z = ih_2$ , has to be mapped onto the point  $\zeta = 1$ . An expansion of  $\zeta$  near  $\zeta = 1$  in terms of  $z$  was considered in the following form

$$\zeta \simeq 1 + qZ^p \quad (10)$$

where  $p$  and  $q$  are constants to be determined and  $Z$  is the value of  $z$  relative to the point  $z = ih_2$  which corresponds to the point  $\zeta = 1$ , i.e.  $Z = z - ih_2$ . On substituting expression (10) into Eq. (4), rearranging and neglecting all higher-order terms in  $Z$ , and since  $\xi_B, \xi_C, \xi_E, \xi_H, \xi_I, \xi_J, K, p$  and  $q$  are all independent of  $Z$ , we obtain

$$\zeta \simeq 1 + \left( \frac{(Z\gamma/2K)^2(1+\xi_I)^2(1+\xi_B)(1-\xi_C)}{(1+\xi_E)^{1+2\alpha}(1+\xi_J)^{1-2\beta}(1+\xi_H)^{1+2\beta}} \right)^{\frac{1}{\gamma}} \quad (11)$$

where  $\gamma = 3 - 2\alpha$ . Similarly, expansions near the points C and J have also been found but in order to save space these expressions are not present. The differential equation (5) could then be integrated numerically using these approximations as initial boundary conditions.

Before mapping  $G_z$  onto  $G_\zeta$  we must first determine the parameters involved in the transformation. The method we applied to determine the parameters involves initial guesses which are used to determine the dimensions of the region  $G_z$ . An iterative procedure is then adopted in which the values of the parameters are modified until the lengths of the room coincide with their given values to some preset degree of accuracy. We now define the method undertaken to determine the lengths of the region.

## 4 Numerical Determination of the Lengths

Initially we assume that the parameters  $\xi_B, \xi_C, \xi_E, \xi_H, \xi_I, \xi_J$  and  $K$  have been assigned approximate values and this corresponds to fixing the dimensions of the region  $G_z$ . The region

$G_z$  is determined by finding the lengths  $h_1, h_2, h_3, h_4, l_1, l_2, l_3$  and  $l_4$  in each case where applicable. As these dimensions are not initially prescribed then an iterative procedure, as outlined later in this section, is required to determine these lengths and their related set of parameters.

To find the distance  $h_1$  the following method is adopted. A real value of  $\zeta$ , less than  $-\xi_H$ , is chosen which ensures that we are along the line HA on the boundary of  $G_z$ . We numerically integrate Eq. (4) vertically downwards using the NAG routine D02BGF, and terminate the integration when the value of  $\eta$  is less than  $-\delta$ , where  $\delta$  is a preassigned small real and positive constant. With  $l_4 < (l_2 + l_3)$ , the point in the  $z$  plane must have just crossed the line CD, and thus we have integrated over a distance  $h_1$ . The other lengths, apart from  $l_4$ , are found using similar methods but using the expansions near the appropriate corners. The length  $l_4$  has to be treated differently since it represents the distance between two parallel lines for which there is no horizontal or vertical line that touches both of these parallel lines, so  $l_4$  is found using the following method. From an expansion near the corner C, an approximation to  $\zeta$  is found for  $z = \delta_0$ . Using the NAG routine D02CJF, the value of  $\zeta$  at  $z = l_a$  is found, where  $l_a$  is a suitable real positive value. This moves the point being considered horizontally further to the right of C. Integrating Eq. (4) vertically upwards a distance  $l_b$ , the value of  $\zeta$  is found, where  $l_b$  is a suitable real positive value. Finally, we integrate horizontally from right to left until the value of  $\eta$  is less than  $-\delta$ , this distance is called  $l_c$ , so that the length  $l_4$  is  $(l_c - l_a)$ . The total path taken by the point being considered in  $G_z$  is represented by the dashed arrowed lines in Fig. 2.

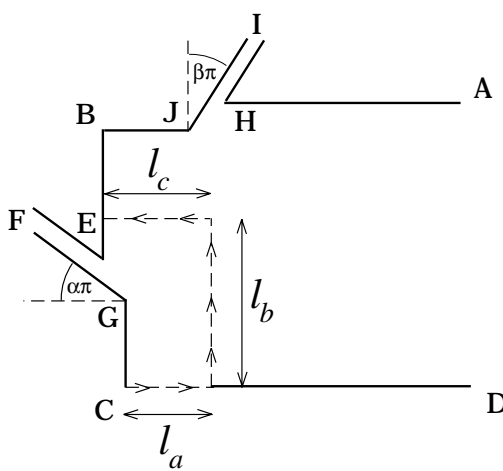


**Figure 2 :** The path taken by the point in  $G_z$  to find the length  $l_4$  with  $h_1 > (h_2 + h_3)$  or  $l_4 < (l_2 + l_3)$ .

## 5 Numerical Determination of the Parameters

The unknown parameters must be determined using an iterative procedure. This method requires initial estimates of the parameters in the differential equation (4) which in turn induces, as discussed above, a set of lengths which define the region  $G_z$ . By slightly changing the values of parameters one at a time, for example  $\xi_B$  to  $\tilde{\xi}_B$ , new sets of lengths are found. The Newton-Raphson method with the Jacobian matrix approximated by a finite-difference quotient matrix is then used to modify the values of the parameters. Iteration continues until the lengths converge to some preset degree of accuracy.

In this investigation we evaluate  $S$ , which is the average value of the square root of the sum of the squares of the calculated lengths from their initial prescribed room values, and when this value is less than  $10^{-5}$  we terminate the iteration procedure. It is found that initially it is advisable to vary all of the parameters by the same small constant amount, e.g. 0.01, but once the value of  $S$  is less than about  $10^{-1}$  then  $\delta\xi_B$  can be taken as  $(\tilde{\xi}_B - \xi_B)/2$ , with similar choices for the other parameters. In order to illustrate this method we assume typical dimensions of the room in the form of the lengths  $H_1, H_2, H_3, L_1, L_2$  and  $L_3$  take the values 3.0m, 1.0m, 0.5m, 4.0m, 1.0m and 0.25m, respectively, and we choose a small set of values of  $\alpha$  and  $\beta$ , see Tab. 1. There are 7 lengths so the matrix involved

**Table 1 :** Typical results from the numerical method for various values of  $\alpha$  and  $\beta$ .

$\alpha = 1/4$	$\alpha = 1/4$	$\alpha = -1/4$	$\alpha = -1/4$
$\beta = 1/3$	$\beta = -1/3$	$\beta = 1/3$	$\beta = -1/3$
$\xi_B$	4.6566	4.6574	16.0312
$\xi_C$	3.1903	3.1905	7.9985
$\xi_E$	0.3488	0.3488	3.1604
$\xi_H$	8.2882	8.3994	27.1501
$\xi_I$	8.0855	7.4397	26.5294
$\xi_J$	7.1806	7.2690	23.7586
$K$	0.9549	0.9549	0.9549

in the Newton-Raphson iteration scheme is a 7 by 7 matrix. For the transformation of complicated regions it is useful to consider a sequence of regions which increase in complexity by the further addition of another sub-channel. This build up to the final region can be useful in establishing suitable first estimates for the unknown parameters of more complicated regions and such details can be found in Trevelyan, Elliott and Ingham (1999).

## 6 Some Analytical Relationships

For each semi-infinite channel an analytical global relationship can be derived which relates the width of the channel to the parameters. These are derived by integrating around semi-circles and letting the radius tend to zero or infinity in the  $\zeta$

plane. We appeal to Cauchy's Theorem to deform the semi-circle to the arc in the  $\zeta$  plane which has been mapped from lines perpendicular to the boundaries in  $G_z$ .

Considering a vertical line which is far right of the top sub-channel in  $G_z$  then this will be mapped to a large arc in  $G_\zeta$ ,  $\Gamma_0$ . Since singular points only occur along the real axis of the  $\zeta$  plane, and given that the large arc avoids them, Cauchy's Theorem means that the integral around this arc is equal to the integral around the semi-circle which has the same end points.

The boundary of the semi-circular arc,  $\Gamma_1$ , of radius  $r_1$ , is given by  $\zeta = r_1 e^{i\theta} + l_o$ , where  $\theta \in [0, \pi]$  and  $l_o$  is the value of  $\zeta$  at the centre of the semi-circle. Hence the integral around the arc  $\Gamma_0$  is given by

$$\int_{\Gamma_0} f_g(\zeta) d\zeta = \int_{\Gamma_1} f_g(\zeta) d\zeta = \int_0^\pi f_g(r_1 e^{i\theta} + l_o) i r_1 e^{i\theta} d\theta \quad (12)$$

On letting  $r_1$  tend to infinity reduces the integral around the arc to

$$\int_0^\pi K i d\theta = i K \pi \quad (13)$$

However, on letting  $r_1$  tend to infinity is equivalent to moving the vertical line an infinite distance to the right. Clearly the height of the vertical line remains constant since the floor and ceiling are parallel. Thus,

$$\int_{\Gamma_0} f_g(\zeta) d\zeta = \int_a^{a+ih_1} dz = ih_1 \quad (14)$$

and hence, we have

$$h_1 = K\pi \quad (15)$$

Similarly, we can consider  $\zeta = r_2 e^{i\theta}$  and let  $r_2$  tend to zero, resulting in

$$h_3 = \sec(\alpha\pi) \frac{K\pi}{\xi_J} \left( \frac{\xi_E \xi_H \xi_J}{\xi_B \xi_C} \right)^{\frac{1}{2}} \xi_E^\alpha \left( \frac{\xi_H}{\xi_J} \right)^\beta \quad (16)$$

and  $\zeta = r_3 e^{i\theta} - \xi_J$  and on letting  $r_3$  tend to zero, we obtain the result

$$l_3 = \sec(\beta\pi) K\pi P^{\frac{1}{2}}$$

$$\text{where } P = \frac{(\xi_J + 1)(\xi_J - \xi_E)^{1+2\alpha}(\xi_J - \xi_J)(\xi_H - \xi_J)^{1+2\beta}}{\xi_J^2(\xi_J + 1)^{2\alpha}(\xi_J + \xi_C)(\xi_J - \xi_B)(\xi_J - \xi_J)^{2\beta}} \quad (17)$$

It was found that the numerical results for the various parameters in the section concerning the Numerical Determination of the Parameters did indeed satisfy the parameter relationships given by Eqs. (15), (16) and (17). If the analytical relationships between the parameters are used within the numerical

method then there are only 4 unknown independent parameters.

If we had considered a sequence of regions of increasing complexity, say by initially denying the existence of the sub-channel at an angle of  $\beta\pi$  to the normal to the channel, then we would have obtained different analytical relationships between the parameters. However, the relevant parameters for the sub-channel at an angle of  $\alpha\pi$  to the normal to the channel would satisfy a similar expression to Eq. (16), which when compared to the full situation gives the approximate relationship that  $\xi_J^2 \simeq \xi_J^{1-2\beta} \xi_H^{1+2\beta}$ , with an error of about 0.1% in  $\xi_J$ .

## 7 Results

Using the NAG routine D02CJF we integrate over a mesh in the  $z$  plane, rotating the planes for the two oblique channels, to map the region  $G_z$  into the  $\zeta$  plane and short distances, typically 0.5m, down the two narrow channels are included. Physically we have investigated the potential flow in a long channel with two ducts, one attached to the top and one attached to an end. The sub-channel attached to the top of the main channel entrains fluid into the main channel whilst the sub-channel attached to the end of the main channel extracts it from there. The opposite end of the main channel is assumed to introduce uniform flow into the channel in order to satisfy the continuity equation.

To model this problem we use a 2D potential flow in which the long room is replaced by a semi-infinite channel and the two finite ducts are replaced by semi-infinite sub-channels. This simplified region is mapped to the region  $G_\zeta$  where sinks and sources are used to model the uniform inlets and outlets. The strength of the sink modelling the extraction is  $\lambda$  and the strength of the source modelling the entrainment is  $\mu$ .

Conformal mappings are such that sources and sinks on the boundary of  $G_z$  map onto the sources and sinks of the same strengths on the boundary of  $G_\zeta$ . In order to solve in  $G_\zeta$ , the upper half of the  $\zeta$  plane, it is necessary to solve in the whole of the  $\zeta$  plane, with image sources and sinks of the appropriate strengths introduced at their complex conjugate points in the lower half plane in order to maintain the real  $\zeta$  axis as a boundary, namely to have no flux of fluid across it.

In the region  $G_\zeta$  a source of strength  $\mu$  is placed at  $\zeta = -\xi_J$ , together with a sink of strength  $\lambda$  placed at the origin, and therefore the complex potential  $W$  in  $G_\zeta$  is given by

$$W(\zeta) = \frac{\mu}{\pi} \ln(\zeta + \xi_J) - \frac{\lambda}{\pi} \ln \zeta \quad (18)$$

To illustrate the results obtained we fix  $\lambda = 1.0$  and  $\mu$  being 2.0, 1.0, 0.5 and -0.5 and show the streamline patterns, see Fig. 3, for various values of  $\alpha$  and  $\beta$ .

## 8 Conclusions

In this paper we have presented an alternative method for calculating the parameters involved in the Schwarz-Christoffel transformation. As in all previous methods, in order to generalise this method to extremely complicated regions with a very large number of parameters requires additional numerical calculations. However, due to the lengths being found using integration in the  $z$  plane, rather than in the  $\zeta$  plane, some analytical relationships between the parameters are available. This allows the number of parameters involved to be reduced by one for each semi-infinite channel. Alternatively, these equations could be used purely to assist with the initial guess. If a sequence of regions of increasing complexity is considered, with semi-infinite channels added one at a time, then in addition to having some global analytical relationships, by comparing the regions in sequence, a good local approximate relationship can be obtained for each semi-infinite channel.

**Acknowledgement:** One of the authors (PMJT) would like to acknowledge the financial support of the Engineering and Physical Sciences Research Council.

## References

- Abdelmalek, M. B.** (1994): Flow in a waterfall with large Froude-number. *J. Comput. Appl. Math.*, vol. 50, pp. 87–98.
- Chaung, J. M.; Gui, Q. Y.; Hsiung, C. C.** (1993): Numerical computation of Schwarz-Christoffel transformation for simply connected unbounded domain. *Comput. Methods Appl. Mech. Engng.*, vol. 105, pp. 93–109.
- Fletcher, B.; Johnson, A. E.** (1992): Containment testing of fume cupboards-I methods. *Ann. Occup. Hyg.*, vol. 36, pp. 239–252.
- Gribnyak, S. T.; Logvinenko, A. V.; Romanenko, V. N.; Fedorovich, A. Y.; Ennan, A. A.** (1991): Numerical investigation of the 2D potential flow of an ideal fluid using the Schwarz-Christoffel integral. *Compt. Maths. Math. Phys.*, vol. 31, pp. 74–79.
- Hassenpflug, W. C.** (1998): Branched channel free-streamlines. *Comput. Methods Appl. Mech. Engng.*, vol. 159, pp. 329–354.
- Minuhin, V. B.** (1993): A general-solution for the field of polygonal electromagnet. *IEEE Trans. Magn.*, vol. 29, pp. 4121–4141.
- Trevelyan, P. M. J.; Elliott, L.; B., I. D.** (1999): Potential flow in a semi-infinite channel with multiple sub-channels using the Schwarz-Christoffel transformation. *Comput. Methods Appl. Mech. Engng.*, vol. accepted for publication.

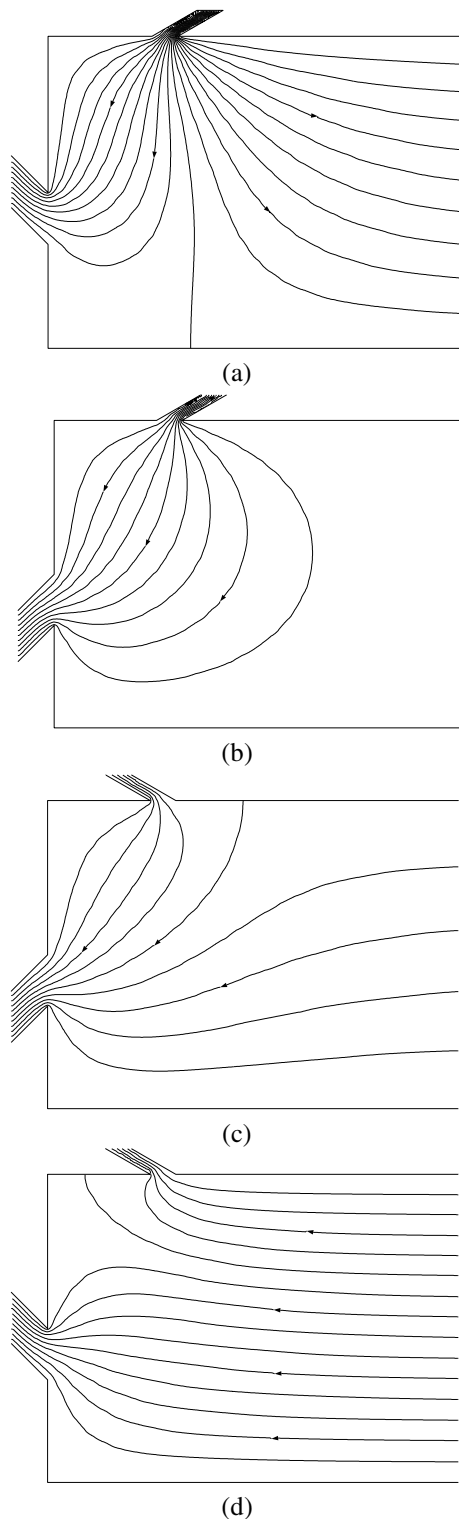


**Figure 3 :** The streamlines for the potential fluid flow with  $\lambda = 1.0$  with  $\mu$  being 2.0, 1.0, 0.5 and -0.5 for various values of  $\alpha$  and  $\beta$ , with the streamlines equally spaced with intervals of 0.1.